Fabrication of titanium carburizing electrodes for capacitive deionization

Wang Li, Lei Lei, Zhou Yun and Fu Jiangtao

ABSTRACT

Titanium carburizing electrodes were used as the electrodes in a capacitive deionization (CDI) process for desalination in this study. Two methods of high vacuum magnetron sputtering and chemical deposition were used for the preparation of nano-titanium carburizing electrodes (named Ti-C* and Ti-C**). By comparing the adsorption capacities of different kinds of electrode material, combined with physical and chemical characteristics and electrochemical analysis, the method of high vacuum magnetron sputtering to prepare Ti-C* electrodes have been proved successful for the CDI process. The results show that under the same conditions, the adsorption capacity of Ti-C* and Ti-C**were 9.6 mg/g and 7.12 mg/g, respectively. The Ti-C* electrodes showed a higher ion electrosorption capacity than Ti-C** and the electrodes can be easily regenerated, indicating excellent recyclability. This study provided a novel method to fabricate titanium carburizing electrodes in CDI process and might lead to the improvement of the CDI desalination performance in an industrial practical application.

Key words | capacitive deionization (CDI), chemical deposition (CD), electrode materials, magnetron sputtering (MS), nano-titanium carburizing electrodes, salty water

Wang Li (corresponding author)
Lei Lei
Zhou Yun
Fu Jiangtao
College of Resources and Environmental Protection,
Wuhan University of Science and Technology,
Wuhan 430081,
China
E-mail: *13657248578@163.com*

INTRODUCTION

Due to breakneck economic growth, urbanization industrial and agricultural activities have taken a great toll on large-scale exploitation and contamination of water resources (Oren 2008). The desalination process converts seawater, brackish water, and salty waste water from industrial processes into affordable fresh water and is one of the key strategic solutions to resolve the severe crisis of water resource shortages (Bouhadana *et al.* 2010).

Several desalination technologies including distillation, reverse osmosis, nano filtration, ion exchange, electrodialysis, membrane distillation, multi-effect distillation, multi-stage flash, and electric desalination have been explored (Gambler & Badreddin 2004; Ba & Economy 2010; Sen *et al.* 2011; Zhao & Zhu 2011; Kang & Cao 2012; Turek *et al.* 2012; Hilal *et al.* 2014; Özgür *et al.* 2014). Capacitive deionization (CDI) has many advantages, such as low energy consumption, low costs for operation and maintenance, and no secondary pollution, and is simple compared with the traditional desalination technologies.

CDI is an electrochemical process for removing salt from aqueous solutions by taking advantage of the excess ions adsorbed in the electrical double layer region at an electrode–solution interface when the electrode is electrically charged by an external power supply (Hou & Huang 2013). The desalination and regeneration process in CDI is shown in Figure 1. The deionization process is shown in Figure 1(a) and the regeneration process in Figure 1(b). It is clear that the electrode is the core component of CDI cells, thus the electrode's electrochemical and physical characteristics are the main influential factors for CDI desalination in aqueous solutions (Welgemoed & Schutte 2005).

Materials mentioned in the paper by Kim & Choi (2010), such as activated carbon, carbon aerogel, carbon nanofibers, and carbon nanotubes can be used as electrosorption electrodes. Although activated carbon can be easily obtained, carbon aerogel, carbon nanofibers, and carbon nanotubes have better electrosorption performance in the electrode surface, electrical conductivity, and specific surface areas. The composite nanomaterials are regarded as attractive candidates for electrode material for CDI. Wang *et al.* (2006) reported the use of carbon nanotubes and nanofibers (CNTs–CNFs) composite film electrodes with a low-cost,

doi: 10.2166/wst.2017.210

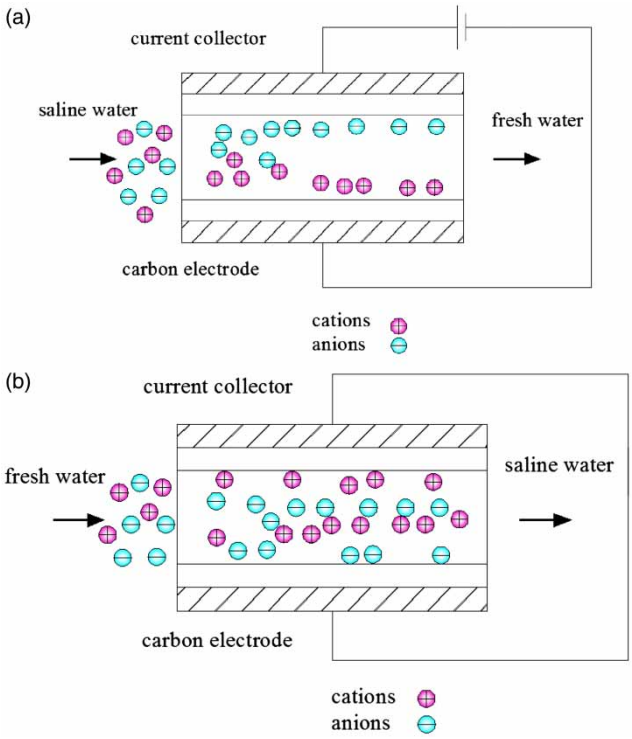

Figure 1 | Schematic diagram of deionization process (a) and regeneration process (b) in CDI.

large area. Pan *et al.* (2009) used carbon nanotube and nanofiber (CNT–CNF) composites as CDI electrode material. The results of these studies are promising with respect to the suitability of CNTs as electrode material. More recently, Peng *et al.* (2013) reported three-dimensional micro/mesoporous carbon composites with carbon nanotube networks for CDI and have shown its high surface area, suitable pore size/volume and special interconnected micro/mesoporous structure, superior electrochemical and CDI performances.

In this study, double interface deposited electric ions nano-titanium carburizing porous electrodes were fabricated. The prepared nano-titanium carburizing electrodes were applied to construct a CDI desalination reactor.

EXPERIMENTAL

Fabrication of nano-titanium carburizing electrodes

Two methods of high vacuum magnetron sputtering and chemical deposition were used for the preparation of nano-titanium carburizing electrodes (named Ti-C* and Ti-C**). The following steps introduce the preparation of the electrode process in detail and the electrode fabrication process is shown in Figure 2:

(1) Titanium sheet polishing by sandpaper: The Ti sheets were cut into 10 mm × 30 mm × 1 mm pieces for use (Baoji Titanium Constant Sharp Titanium Anode Products Co., Ltd, Bao Ji, China). The surface of the Ti sheets was polished to be flat and smooth with sandpapers of 500 mesh, 800 mesh, 1,200 mesh, and 1,500 mesh.
(2) Polishing by polishing liquid: The sample Ti sheets were ultrasonically cleaned in acetone (to remove the oil on the surface), ethanol (to remove the acetone), and deionized water (DI) water (to remove the ethanol) for 3 min. Then, they were chemically polished with polishing liquid (volume ratio of H_2O, HNO_3, and HF was 5:4:1), ultrasonically cleaned for 10 s in the polishing liquid and washed with DI water for 5 min. The sample Ti pieces were dried in an oven and stored in a vacuum dryer.
(3) Anodization by electrochemical methods: The preparation of TiO_2 nanotube arrays by the anodic oxidation method used flake graphite as the cathode and the sample Ti sheets in step (2) as anode. Two electrodes were placed in parallel in a beaker of electrolyte, and voltage was applied on the electrodes. The electrolyte contained the volume fraction of 90% glycol, 5%

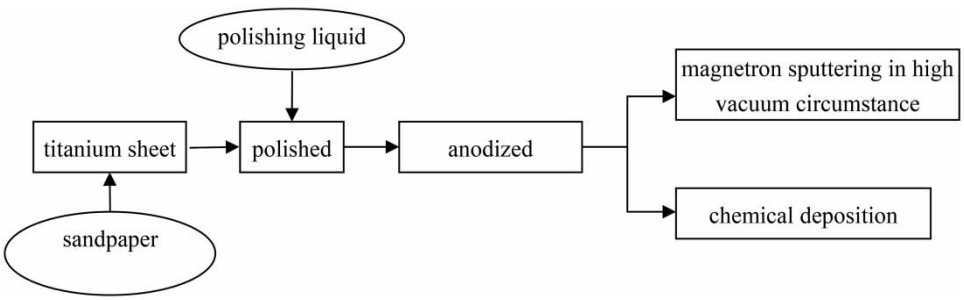

Figure 2 | The electrode fabrication process.

methanol, 5% of the DI water, and the mass fraction of 0.5% ammonium fluoride. The whole device was put into a constant temperature heating magnetic stirrer and stirred at 25 °C at 100 rpm.

TiO_2 nanotube arrays with different lengths and different diameters were made with the parameter (voltages, the voltage boost rate, and anodizing time) changes during the anodizing process. In this experiment, the voltage boost rate was 0.1 V/s, starting from 0 V to 5 V and maintained for 3 min, and then from 5 V to 60 V to find the maximum current and maintained for 45 min. To end the anodizing process the high speed and high precision DC programmable power supply was turned off. The anodizing electrodes were taken from the electrolyte and rinsed immediately with DI water, then the dry electrode samples were stored in the vacuum dryer.

(4) Magnetron sputtering in high vacuum circumstances: The sample anodization Ti sheets from step (3) were ultrasonically cleaned in acetone and ethanol for 5 min, then washed in DI water and dried with a rubber suction bulb. In this study, a FJL500 type high-vacuum multi-functional magnetic control and ion sputtering apparatus were used. With graphite (purity 99.999%) as the target, Ar (flow rate of 36 sccm) as the sputtering gas, the sputtering power was 200 W, and the working air pressure 1.2 Pa. The sample was cooled down under the protection of nitrogen and labeled as Ti-C*.

(5) Chemical deposition: The anodization Ti sheets from step (3) were put in a vacuum tube furnace filled with argon. Then under the protection of 15 L/min argon, the temperature was increased to 850 °C with a temperature boost rate of 15 °C/min. Then, the argon was changed to acetone atmosphere, to make it pass an acetone solution. The acetone was put into a reaction chamber and reacted for 2 h. After the reaction was finished, natural cooling to room temperature under the protection of argon took place. Then, the samples were removed and ultrasonically cleaned in DI water for 2 min, ethanol for 2 min, then washed in DI water and dried with a rubber suction bulb. The sample was labeled as Ti-C**.

Desalination experiments

The experimental process of the CDI desalination system consisted of a beaker, a peristaltic pump, a flow meter, a CDI unit, a DC power supply, and a conductivity meter. Two kinds of electrodes, Ti-C** and Ti-C*, were installed into the CDI unit separately for salty water desalination experiments. The effective mass of the electrode material was 1.24 g. The NaCl solution concentration was 50 mg/L (electronic conductivity was 129 μs/cm), the total liquid volume was 100 mL with a flow rate of 10 mL/min, the space between electrodes was 4 mm, the inlet flow rate was 20 mL/min, and the working voltage was 1.4 V. The conductivity of the solution was measured at regular intervals by a conductivity meter. The desalination efficiency was calculated according to the following formula:

$$\eta = \frac{C_0 - C_t}{C_0} \times 100\% \quad (1)$$

where η is the desalination efficiency, C_0 is the initial conductivity, and C_t is the saturation conductivity.

Measurements

The surface morphology characteristics of Ti-C* and Ti-C**electrodes were observed by scanning electron microscope (Nova 400 Nano SEM, FEI, Hillsboro, USA). The Brunauer–Emmett–Teller (BET) specific surface areas of Ti-C* and Ti-C**electrodes were measured by surface area and pore size distribution analyzer (ASAP2020, Micromeritics Instrument Corporation, Quantachrome Instruments, USA). Cyclic voltammetry (CV) curves and AC impedance spectra were obtained by using a CHI660E electrochemical workstation (Shanghai CH Instruments Co. Ltd, Shanghai, China).

RESULTS AND DISCUSSION

Characterization of Ti-C** and Ti-C* materials

Surface characterization

The SEM images of the Ti-C** and Ti-C* surface are shown in Figure 3(a) and 3(b), respectively. Spectrum 1 and Spectrum 2 are the energy dispersive X-ray spectroscopy (EDS) energy spectrum of Ti-C*. The surface morphology of these two kinds of electrodes can be clearly seen from the 100,000 times' magnification, which is arranged in neat arrays of nanotubes, and provides a large specific surface area for ion adsorption. The nano-titanium tube electrode surface of Ti-C* was covered with an uneven arrangement of carbon balls, which increased the available surface area for adsorption. In the EDS energy spectrum, there are

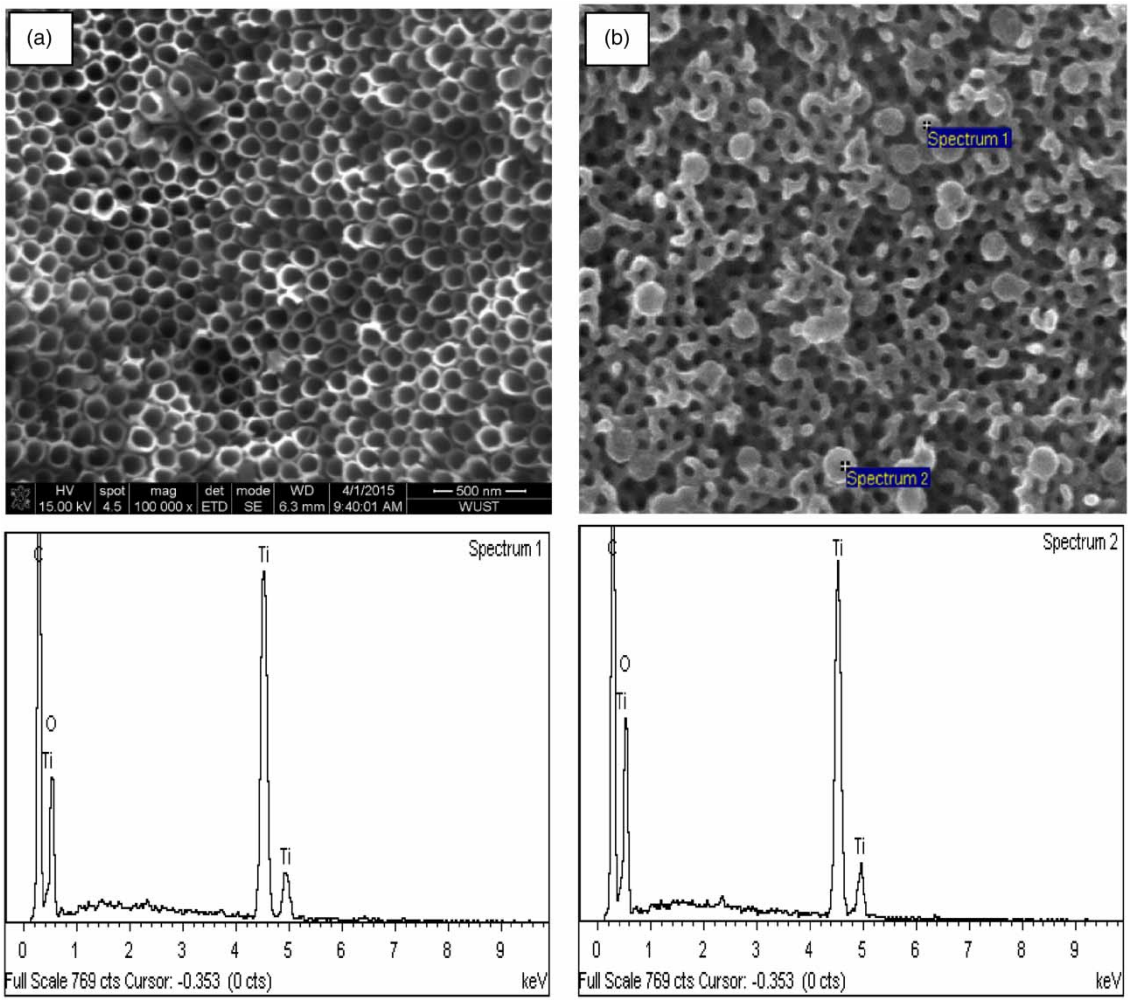

Figure 3 | SEM images of electrode materials: (a) Ti-C** and (b) Ti-C*; Spectrum 1 and Spectrum 2 are the EDS energy spectrum diagram of Ti-C* material.

obvious C signals besides the Ti and O signals. Therefore, it is clear that the magnetron sputtering in high vacuum circumstances and chemical deposition methods are feasible for CDI electrode fabrication.

BET specific surface area

The BET specific surface areas of the Ti-C** and Ti-C* electrodes were measured as 448 m^2/g and 117 m^2/g, respectively, by the N2 adsorption/desorption isotherm. The results show that the pores are mainly constituted of micro-pores.

The results show a slight decrease of the BET specific surface area for the PPy/CNT electrode, which is probably because the wrapping of the PPy layer on the CNTs increases the diameter of the nanotube composites.

Characterization of Ti-C** and Ti-C* electrodes

Cyclic voltammetry curves

In the measurements, the titanium carburizing electrodes were used as the working electrode, while a saturated calomel electrode and a Pt electrode were used as the reference and counterpart electrode, respectively. The electrolyte solution was 0.5 mol/L NaCl. The CV measurement was performed in a potential range of 0 to 1.0 V with scanning speed of 2 mV/s, 5 mV/s, 10 mV/s, and 30 mV/s.

Figure 4(a) and 4(b) show the two samples, Ti-C* and Ti-C**. The calculated average specific capacitance value of the electrodes evaluated by Equation (2) can be seen in Table 1. At lower scanning speed, the pulse voltage has

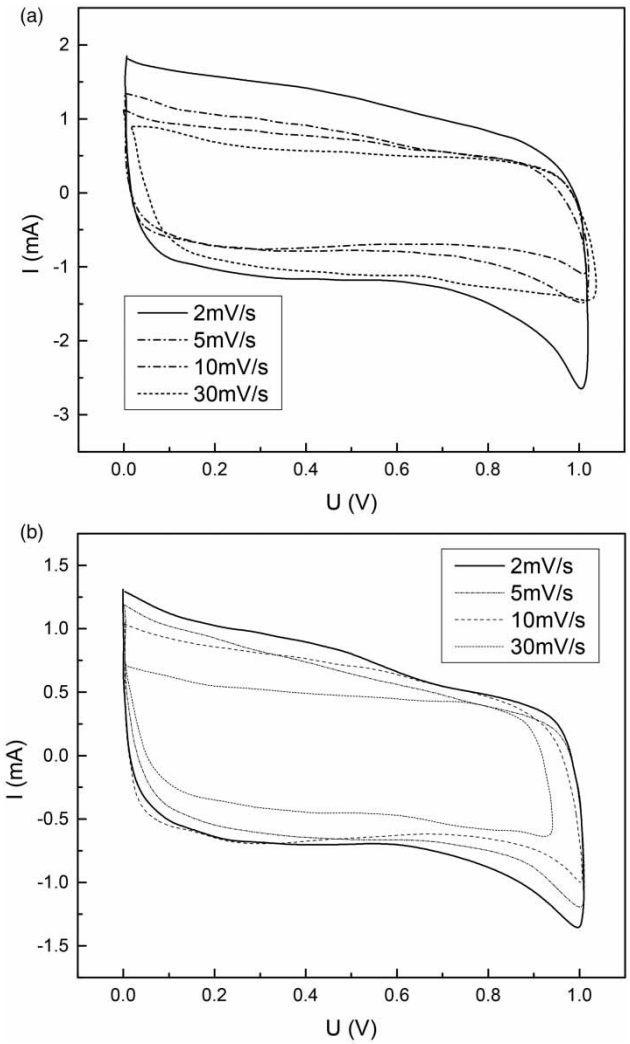

Figure 4 | The CV curves of Ti-C* and Ti-C**.

Table 1 | Calculated average specific capacitance value of the electrodes

	Scanning speed			
Electrodes	**2 mV/s**	**5 mV/s**	**10 mV/s**	**30 mV/s**
Ti-C*	56.2 F/g	41.9 F/g	28.3 F/g	10.4 F/g
Ti-C**	45.1 F/g	30.9 F/g	16.2 F/g	7.5 F/g

relatively more time in the pores of the electrode, and the average amount of capacitance is larger.

$$C = \frac{\int_{E_1}^{E_2} i(E)dE}{(E_2 - E_1)/mv} \quad (2)$$

where E_1, E_2 (V) are the initial and final potential, respectively, i(E) is the response current, v (V/s) is the potential scan rate, and m (g) is the mass of active component in the electrode.

Comparing the CV curves and average specific capacitance value of the two different electrode materials, the specific capacitance value of Ti-C* was larger than Ti-C**. The CV curves showed good rectangular characteristics, showing a typical double layer capacitance characteristic. It can be concluded that under the action of electric field force, it can form a stable electric double layer, and the electrode's charge and discharge performance is excellent.

AC impedance spectra

The AC impedance spectra of the Ti-C* and Ti-C** electrodes were tested by the CHI660E electrochemical workstation with a three electrodes system. The working electrode had a surface area of 1 cm^2. The electrolyte solution was 0.5 mol/L NaCl, and the frequency range was between 0.01 Hz and 100 KHz. The AC impedance spectra of Ti-C* and Ti-C** are shown in Figure 5.

As shown in Figure 5, the AC impedance spectra curve of Ti-C* was almost a straight line in the high frequency area, and the AC impedance spectra curve of Ti-C** was a large semicircle in the high frequency area. This implied that the diffusion resistance of the ions in the interface of the liquid and Ti-C** electrode was greater than for Ti-C*. In the low frequency area, the electrolyte ion diffusion resistance was represented by the straight part in the horizontal projection of the internal electrode resistance. The electrical characteristics of the Ti-C* electrode are close to that of pure capacitance. The diffusion resistance of ions in the Ti-C* electrodes is less than Ti-C**.

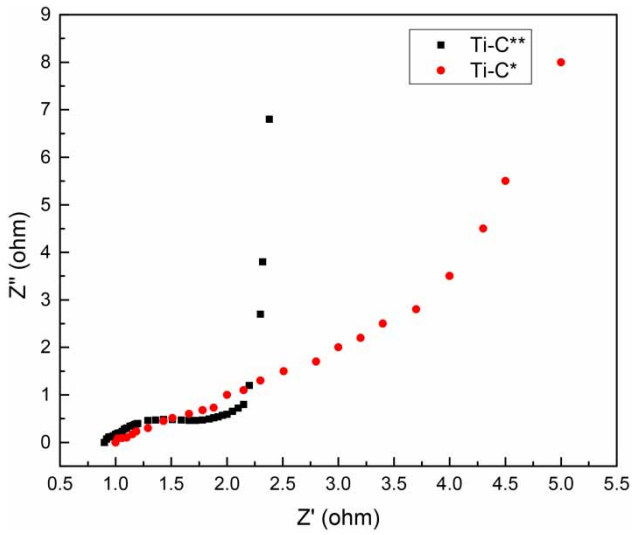

Figure 5 | AC impedance spectra of Ti-C* and Ti-C** electrodes.

Desalting performances by Ti-C** and Ti-C* in CDI process

Two kinds of electrodes, Ti-C** and Ti-C*, were installed into the CDI unit separately for salty water desalination experiments. As shown in Figure 6, desalination ability increased with the increase of running time, the conductivity of salt decreased from 129 μs/cm to 68 μs/cm in 37 min in the Ti-C* CDI unit; the desalination rate reached 47.3%, and the desalination rate in the Ti-C** CDI unit reached 35.0% at the same operational parameters. The adsorption capacity of the two electrodes was calculated, that of the Ti-C* electrode was 9.61 mg/g, and the adsorption capacity of the Ti-C** electrode was 7.11 mg/g. In the process of CDI, the electrode material with higher capacitance has a higher salt removal efficiency.

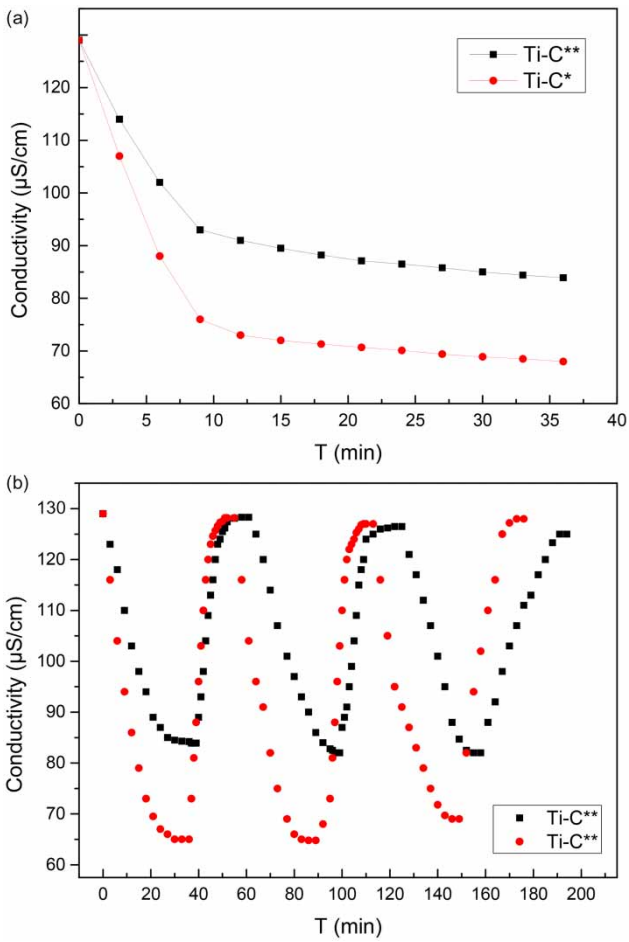

Figure 6 | CDI performance of Ti-C* and Ti-C** electrodes: (a) saturated adsorbing curve of Ti-C* and Ti-C** electrodes; (b) the absorption/desorption cycles of Ti-C* and Ti-C**.

Further, the regeneration performance of Ti-C* and Ti-C** electrodes is excellent. Figure 6(b) shows three successive runs of absorption/desorption cycles. The regeneration of Ti-C* and Ti-C** electrodes was obtained at almost 100%. Ti-C* demonstrates a better recyclability than Ti-C**. It can be seen that the good performance of Ti-C* and Ti-C** cells could be maintained for multiple cycling operations. Hence, Ti-C* and Ti-C** electrodes have great potential as high-performance cathode material for CDI technology.

CONCLUSIONS

In this study, two ways were presented to fabricate titanium carburizing electrodes for CDI. As shown in the SEM, the two materials were covered with an uneven arrangement of carbon balls. The surface area and pore size distribution analyser test suggested the advantages of a large specific surface area and developed pores. In the electrochemical test, the Ti-C* and Ti-C** electrodes showed a high specific capacity and good charge–discharge properties and impedance characteristics. In addition, the Ti-C* electrodes showed a higher ion electrosorption capacity than Ti-C** and the electrodes can be easily regenerated, indicating excellent recyclability. The adsorption capacity of the Ti-C* electrode was 9.61 mg/g and the desalination efficiency was 47.3%. The two electrodes both had a good cycle performance. Hence, the Ti-C* composite was demonstrated to be a promising cathode material for CDI technology.

ACKNOWLEDGEMENTS

This study was supported by the National Science and Technology Ministry (2015BAB18B00), Wuhan, China.

REFERENCES

Ba, C. & Economy, J. 2010 Preparation and characterization of a neutrally charged antifouling nanofiltration membrane by coating a layer of sulfonated poly(ether ether ketone) on a positively charged nanofiltration membrane. *Journal of Membrane Science* **362** (1–2), 192–201.

Bouhadana, Y., Avraham, E., Soffer, A. & Aurbach, D. 2010 Several basic and practical aspects related to electrochemical deionization of water. *AIChE Journal* **56** (3), 779–789.

Gambler, A. & Badreddin, E. 2004 Dynamic modelling of MSF plants for automatic control and simulation purposes: a survey. *Desalination* **166** (1), 191–204.

Hilal, N., Kochkodan, V., Abdulgader, H. A., Mandale, S. & Al-Jlil, S. A. 2014 A combined ion exchange–nanofiltration process for water desalination: I. Sulphate–chloride ion-exchange in saline solutions. *Desalination* **363**, 44–50.

Hou, C. H. & Huang, C. Y. 2013 A comparative study of electrosorption selectivity of ions by activated carbon electrodes in capacitive deionization. *Desalination* **314** (8), 124–129.

Kang, G. D. & Cao, Y. M. 2012 Development of antifouling reverse osmosis membranes for water treatment: a review. *Water Research* **46** (3), 584–600.

Kim, Y. J. & Choi, J. H. 2010 Enhanced desalination efficiency in capacitive deionization with an ion-selective membrane. *Separation & Purification Technology* **71** (1), 70–75.

Oren, Y. 2008 Capacitive deionization (CDI) for desalination and water treatment – past, present and future. *Desalination* **228** (1–3), 10–29.

Özgür, A., Ümran, Y., Kabay, N. & Yüksel, M. 2014 Various applications of electrodeionization (EDI) method for water treatment – a short review. *Desalination* **342** (5), 16–22.

Pan, L., Wang, X., Gao, Y., Zhang, Y., Chen, Y. & Sun, Z. 2009 Electrosorption of anions with carbon nanotube and nanofibre composite film electrodes. *Desalination* **244** (1), 139–143.

Peng, Z., Zhang, D., Yan, T., Zhang, J. & Shi, L. 2013 Three-dimensional micro/mesoporous carbon composites with carbon nanotube networks for capacitive deionization. *Applied Surface Science* **282** (10), 965–973.

Sen, P. K., Sen, P. V., Mudgal, A. & Singh, S. N. 2011 A small scale multi-effect distillation (MED) unit for rural micro enterprises: part-III heat transfer aspects. *Desalination* **279** (1–3), 15–26.

Turek, M., Was, J. & Dydo, P. 2012 Brackish water desalination in RO–single pass EDR system. *Desalination & Water Treatment* **7** (1), 263–266.

Wang, X. Z., Li, M. G., Chen, Y. W., Cheng, R. M., Huang, S. M., Pan, L. K. & Sun, Z. 2006 Electrosorption of NaCl solutions with carbon nanotubes and nanofibers composite film electrodes. *Electrochemical and Solid-State Letters* **9** (9), E23–E26.

Welgemoed, T. J. & Schutte, C. F. 2005 Capacitive deionization technology™: an alternative desalination solution. *Desalination* **183** (1), 327–340.

Zhao, Z. P. & Zhu, C. Y. 2011 Concentration of ginseng extracts aqueous solution by vacuum membrane distillation. 2. Theory analysis of critical operating conditions and experimental confirmation. *Desalination* **267** (2–3), 147–153.

First received 30 November 2016; accepted in revised form 28 March 2017. Available online 20 April 2017